Inorg. Chem. **2008**, *47*, 7908−7913

Mononuclear Nickel(III) Complexes $[Ni^{III}(OR)(P(C_6H_3\text{-}3\text{-}SiMe_3\text{-}2\text{-}S)_3)]^-$ (R = Me, Ph) Containing the Terminal Alkoxide Ligand: Relevance to the Nickel Site of Oxidized-Form [NiFe] Hydrogenases

Tzung-Wen Chiou and Wen-Feng Liaw*

Department of Chemistry, National Tsing Hua University, Hsinchu 30043, Taiwan

Received March 31, 2008

The unprecedented nickel(III) thiolate $[Ni^{III}(OR)(P(C_6H_3\text{-}3\text{-}SiMe_3\text{-}2\text{-}S)_3)]^-$ [R = Ph (**1**), Me (**3**)] containing the terminal Ni^{III}−OR bond, characterized by UV−vis, electron paramagnetic resonance, cyclic voltammetry, and single-crystal X-ray diffraction, were isolated from the reaction of $[Ni^{III}(Cl)(P(C_6H_3\text{-}3\text{-}SiMe_3\text{-}2\text{-}S)_3)]^-$ with 3 equiv of [Na][OPh] in tetrahydrofuran (THF)−CH_3CN and the reaction of complex **1** with 1 equiv of $[Bu_4N][OMe]$ in THF−CH_3OH, respectively. Interestingly, the addition of complex **1** into the THF−CH_3OH solution of $[Me_4N][OH]$ also yielded complex **3**. In contrast to the inertness of complex $[Ni^{III}(Cl)(P(C_6H_3\text{-}3\text{-}SiMe_3\text{-}2\text{-}S)_3)]^-$ toward 1 equiv of [Na][OPh], the addition of 1 equiv of [Na][OMe] into a THF−CH_3CN solution of $[Ni^{III}(Cl)(P(C_6H_3\text{-}3\text{-}SiMe_3\text{-}2\text{-}S)_3)]^-$ yielded the known $[Ni^{III}(CH_2CN)(P(C_6H_3\text{-}3\text{-}SiMe_3\text{-}2\text{-}S)_3)]^-$ (**4**). At 77 K, complexes **1** and **3** exhibit a rhombic signal with *g* values of 2.31, 2.09, and 2.00 and of 2.28, 2.04, and 2.00, respectively, the characteristic *g* values of the known trigonal-bipyramidal Ni^{III} $[Ni^{III}(L)(P(C_6H_3\text{-}3\text{-}SiMe_3\text{-}2\text{-}S)_3)]^-$ (L = SePh, SEt, Cl) complexes. Compared to complexes $[Ni^{III}(EPh)(P(C_6H_3\text{-}3\text{-}SiMe_3\text{-}2\text{-}S)_3)]^-$ [E = S (**2**), Se] dominated by one intense absorption band at 592 and 590 nm, respectively, the electronic spectrum of complex **1** coordinated by the less electron-donating phenoxide ligand displays a red shift to 603 nm. In a comparison of the Ni^{III}−OMe bond length of 1.885(2) Å found in complex **3**, the longer Ni^{III}−OPh bond distance of 1.910(3) Å found in complex **1** may be attributed to the absence of σ and π donation from the [OPh]-coordinated ligand to the Ni^{III} center.

Introduction

Hydrogenase, a metalloenzyme, catalyzes a reversible two-electron oxidation of H_2 in aerobic and anaerobic microorganisms.[1–3] Two classes of hydrogenases, [Fe]-only hydrogenases ([Fe]-only H_2ases) and [NiFe] hydrogenases ([NiFe] H_2ases), have been studied widely. The X-ray crystallographic studies of the active-site structure of [NiFe] H_2ases isolated from *Desulfovibrio gigas*, *Desulfovibrio vulgaris*, *Desulfovibrio fructosovorans*, and *Desulfovibrio desulfuricans* ATCC27774 in combination with infrared spectroscopy have revealed an active site comprised of a heterobimetallic $(S_{cys})_2Ni(\mu\text{-}S_{cys})_2(\mu\text{-}X)Fe(CO)(CN)_2$ ($X = O^{2-}$, HO_2^-, OH^-) cluster.[2,3] The bridging ligand X was proposed to be an oxide, hydroxide, or hydroperoxide in the oxidized state and was found to be absent in the reduced state. Extended X-ray absorption fine structure (EXAFS) studies of *Chromatium*

* To whom correspondence should be addressed. E-mail: wfliaw@mx.nthu.edu.tw.

(1) (a) Carepo, M.; Tierney, D. L.; Brondino, C. D.; Yang, T. C.; Pamplona, A.; Telser, J.; Moura, I.; Moura, J. J. G.; Hoffman, B. M. *J. Am. Chem. Soc.* **2002**, *124*, 281–286. (b) Whitehead, J. P.; Gurbiel, R. J.; Bagyinka, C.; Hoffman, B. M.; Maroney, M. J. *J. Am. Chem. Soc.* **1993**, *115*, 5629–5635. (c) Adams, M. W. W.; Stiefel, E. I. *Curr. Opin. Chem. Biol.* **2000**, *4*, 214–220.

(2) (a) Volbeda, A.; Charon, M. H.; Piras, C.; Hatchikian, E. C.; Frey, M.; Fontecilla-Camps, J. C. *Nature* **1995**, *373*, 580–587. (b) Garcin, E.; Vernede, X.; Hatchikian, E. C.; Volbeda, A.; Frey, M.; Fontecilla-Camps, J.-C. *Structure* **1999**, *7*, 557–566. (c) Ogata, H.; Mizoguchi, Y.; Mizuno, N.; Miki, K.; Adachi, S.-I.; Yasuoka, N.; Yagi, T.; Yamauchi, O.; Hirota, S.; Higuchi, Y. *J. Am. Chem. Soc.* **2002**, *124*, 11628–11635. (d) Foerster, S.; Stein, M.; Brecht, M.; Ogata, H.; Higuchi, Y.; Lubitz, W,. *J. Am. Chem. Soc.* **2003**, *125*, 83–93. (e) Davidson, G.; Choudhury, S. B.; Gu, Z.; Bose, K.; Roseboom, W.; Albracht, S. P. J.; Maroney, M. J. *Biochemistry* **2000**, *39*, 7468–7479. (f) Gu, Z.; Dong, J.; Allan, C. B.; Choudhury, S. B.; Franco, R.; Moura, J. J. G.; Moura, I.; LeGall, J.; Przybyla, A. E.; Roseboom, W.; Albracht, S. P. J.; Axley, M. J.; Scott, R. A.; Maroney, M. J. *J. Am. Chem. Soc.* **1996**, *118*, 11155–11165. (g) Carepo, M.; Tierney, D. L.; Brondino, C. D.; Yang, T. C.; Pamplona, A.; Telser, J.; Moura, I.; Moura, J. J. G.; Hoffman, B. M. *J. Am. Chem. Soc.* **2002**, *124*, 281–286.

(3) (a) Rousset, M.; Montet, Y.; Guigliarelli, B.; Forget, A.; Asso, M.; Bertrand, P.; Fontecilla-Camps, J. C.; Hatchikian, E. C. *Proc. Natl. Acad. Sci. U.S.A.* **1998**, *95*, 11625–11630. (b) Matias, P. M.; Soares, C. M.; Saraiva, L. M.; Coelho, R.; Morais, J.; Le Gall, J.; Carrondo, M. A. *J. Biol. Inorg. Chem* **2001**, *6*, 63–81.

10.1021/ic801069t CCC: $40.75
Published on Web 08/02/2008

vinosum showed that the Ni−O distance of 1.91 Å is consistent with a hydroxy bridge (Ni−A state).[2] The coordination environment about Ni in the [NiFe] H_2ases is pseudo square pyramidal in the oxidized state. The Ni site has been proposed to be redox-active and changes between Ni^{III} and Ni^{II}, while the Fe site remains as Fe^{II} in all spectrally defined redox states of the enzyme.[2–5] The EXAFS/electron paramagnetic resonance (EPR) studies indicate that the formal oxidation state of the Ni center is paramagnetic Ni^{III} in Ni−A, Ni−B, and Ni−C states.[2–5] Also, the ENDOR experiments showed that the Ni−A form exhibits an ^{17}O signal from a solvent-derived ($H_2{}^{17}O$) species, and the signal disappears upon redox cycling to the Ni−C state.[2g] In particular, recent X-ray absorption spectroscopy shows that the Ni site of the regulatory hydrogenase (RH) in the presence of hydrogen (RH^{+H_2}), proposed as the Ni−C state, isolated from *Ralstonia eutropha* is a six-coordinate $[Ni^{III}S_2(O/N)_3(H)]$.[4]

Despite a number of well-characterized high-valent dinuclear bis(μ-oxo)nickel(III) complexes,[5] no mononuclear nickel(III) thiolate complexes containing the terminal alkoxide ligand were reported.[6] Recently, we reported the isolation and characterization of the mononuclear [Ni^{III}(L)(P(C$_6$H$_3$-3-SiMe$_3$-2-S)$_3$)]$^-$ (L = 2-S-C$_4$H$_3$S, SePh, SEt, Cl).[7] The increased electron density of the Ni center of complexes [Ni^{III}(L)(P(C$_6$H$_3$-3-SiMe$_3$-2-S)$_3$)]$^-$ modulated by the monodentate ligand L and the substituted groups of the phenylthiolate rings promotes the stability of the nickel(III) thiolate complexes. The similarity of the synthesized [Ni^{III}(SR)(P(C$_6$H$_3$-3-SiMe$_3$-2-S)$_3$)]$^-$ complexes to the nickel active-site structure of [NiFe] H_2ases has inspired the preparation of derivatives to mimic the features of the Ni−A and Ni−B states of the catalytic cycle of [NiFe] H_2ase. Herein, we report the synthesis of [Ni^{III}(OR)(P(C$_6$H$_3$-3-SiMe$_3$-2-S)$_3$)]$^-$ [R = Ph (**1**), Me (**3**)] containing the terminal Ni^{III}−OPh and Ni^{III}−OMe bonds, respectively.

Results and Discussion

In contrast to the inertness of [Ni^{III}(Cl)(P(C$_6$H$_3$-3-SiMe$_3$-2-S)$_3$)]$^-$ toward 1 equiv of [Na][OPh] in tetrahydrofuran (THF)−CH_3CN (3:1 volume ratio) at room temperature, [Ni^{III}(Cl)(P(C$_6$H$_3$-3-SiMe$_3$-2-S)$_3$)]$^-$ and 3 equiv of [Na][OPh] dissolved in THF−CH_3CN (3:1 volume ratio) were stirred at ambient temperature for 12 h to yield the mononuclear [Ni^{III}(OPh)(P(C$_6$H$_3$-3-SiMe$_3$-2-S)$_3$)]$^-$ (**1**; yield 73%) after separation of the insoluble NaCl and the excess [Na][OPh] by filtration (Scheme 1a).[7] Complex **1** is air-stable in the solid state and exhibits a diagnostic ^1H NMR spectrum with phenyl proton resonances well removed from the diamagnetic region. The proton resonances [δ 15.8 (br), 10.4 (br), 9.4 (br), −5.3 (br) ppm] were assigned to [OPh]$^-$ and [P(C$_6$H$_3$-3-SiMe$_3$-2-S)$_3$]$^{3-}$ ligands. Compared to the rhombic signal with g values of 2.31, 2.09, and 2.00 (4.2 K) observed in [Ni^{III}(SePh)(P(*o*-C$_6$H$_3$-2-S)$_3$)]$^-$,[7a] complex **1** displays a rhombic signal with g values of 2.31, 2.04, and 1.99 [THF−CH_3CN (3:1 volume ratio)] at 77 K and g values of 2.28, 2.09, and 2.02 in a powdered sample EPR spectrum (Figure 1). The effective magnetic moment was 1.73 μ_B for complex **1**. These results are consistent with the central Ni^{III} possessing a d^7 electronic configuration in a trigonal-bipyramidal ligand field.[7]

Scheme 1

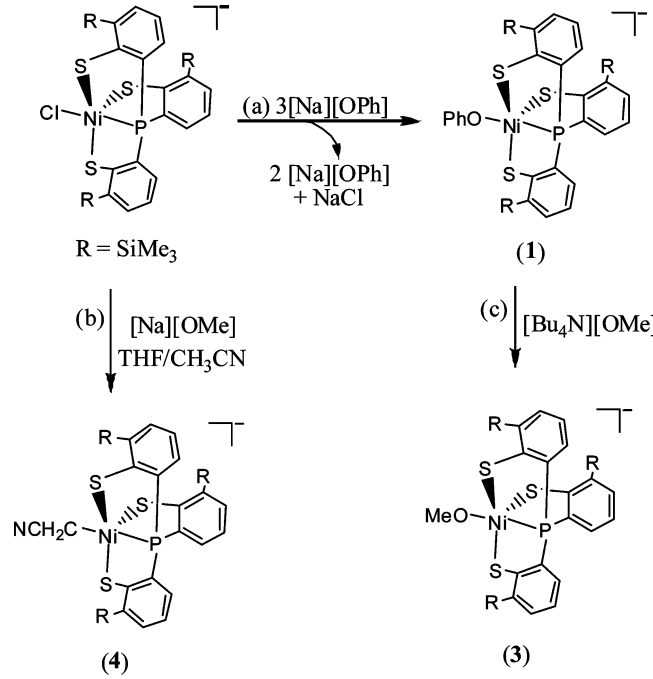

In contrast, upon the addition of 1 equiv of a [Na][SPh] to the THF−CH_3CN (3:1 volume ratio) solution of [Ni^{III}(Cl)(P(C$_6$H$_3$-3-SiMe$_3$-2-S)$_3$)]$^-$, a pronounced color change from dark green to blue green occurs at ambient temperature. The UV−vis, EPR, and single-crystal X-ray diffraction studies confirmed the formation of [Ni^{III}(SPh)(P(C$_6$H$_3$-3-SiMe$_3$-2-S)$_3$)]$^-$ (**2**; Figure 2). Presumably, the stronger σ- and π-electron-donating nature of phenylthiolate [SPh]$^-$, compared to phenoxide [OPh]$^-$, rendering the Ni^{III} center of the [Ni^{III}(P(C$_6$H$_3$-3-SiMe$_3$-2-S)$_3$)]$^-$ motif in the more electron-rich functionality to promote the stability of complex **2** is responsible for the facile formation of complex **2** when [Ni^{III}(Cl)(P(C$_6$H$_3$-3-SiMe$_3$-2-S)$_3$)]$^-$ was reacted with 1 equiv of [Na][SPh] in THF−CH_3CN. In comparison with complex

(4) (a) Haumann, M.; Porthum, A.; Buhrke, T.; Liebisch, P.; Meyer-Klaucke, W.; Friedrich, B.; Dau, H. *Biochemistry* **2003**, *42*, 11004–11015. (b) Brecht, M.; Gastel, M. V.; Buhrke, T.; Friedrich, B.; Lubitz, W. *J. Am. Chem. Soc.* **2003**, *125*, 13075–13083.

(5) (a) Hikichi, S.; Yoshizawa, M.; Sasakura, Y.; Akita, M.; Moro-oka, Y. *J. Am. Chem. Soc.* **1998**, *120*, 10567–10568. (b) Shiren, K.; Ogo, S.; Fujinami, S.; Hayashi, H.; Suzuki, M.; Uehara, A.; Watanabe, Y.; Moro-oka, Y. *J. Am. Chem. Soc.* **2000**, *122*, 254–262. (c) Mandimutsira, B. S.; Yamarik, J. L.; Brunold, T. C.; Gu, W.; Cramer, S. P.; Riordan, C. G. *J. Am. Chem. Soc.* **2001**, *123*, 9194–9195.

(6) (a) Li, Z.; Ohki, Y.; Tatsumi, K. *J. Am. Chem. Soc.* **2005**, *127*, 8950–8951. (b) Zhu, W.; Marr, A. C.; Wang, Q.; Neese, F.; Spencer, D. J. E.; Blake, A. J.; Cooke, P. A.; Wilson, C.; Schröder, M. *Proc. Natl. Acad. Sci. U.S.A.* **2005**, *102*, 18280–18285. (c) Ogo, S.; Kabe, R.; Uehara, K.; Kure, B.; Nishimura, T.; Menon, S. C.; Harada, R.; Fukuzumi, S.; Higuchi, Y.; Ohhara, T.; Tamada, T.; Kuroki, R. *Science* **2007**, *316*, 585–587.

(7) (a) Lee, C.-M.; Chen, C.-H.; Ke, S.-C.; Lee, G.-H.; Liaw, W.-F. *J. Am. Chem. Soc.* **2004**, *126*, 8406–8412. (b) Chen, C.-H.; Lee, G.-H.; Liaw, W.-F. *Inorg. Chem.* **2006**, *45*, 2307–2316. (c) Lee, C.-M.; Chuang, Y.-L.; Chiang, C.-Y.; Lee, G.-H.; Liaw, W.-F. *Inorg. Chem.* **2006**, *45*, 10895–10904. (d) Lee, C.-M.; Chiou, T.-W.; Chen, H.-H.; Chiang, C.-Y.; Kuo, T.-S.; Liaw, W.-F. *Inorg. Chem.* **2007**, *46*, 8913–8923.

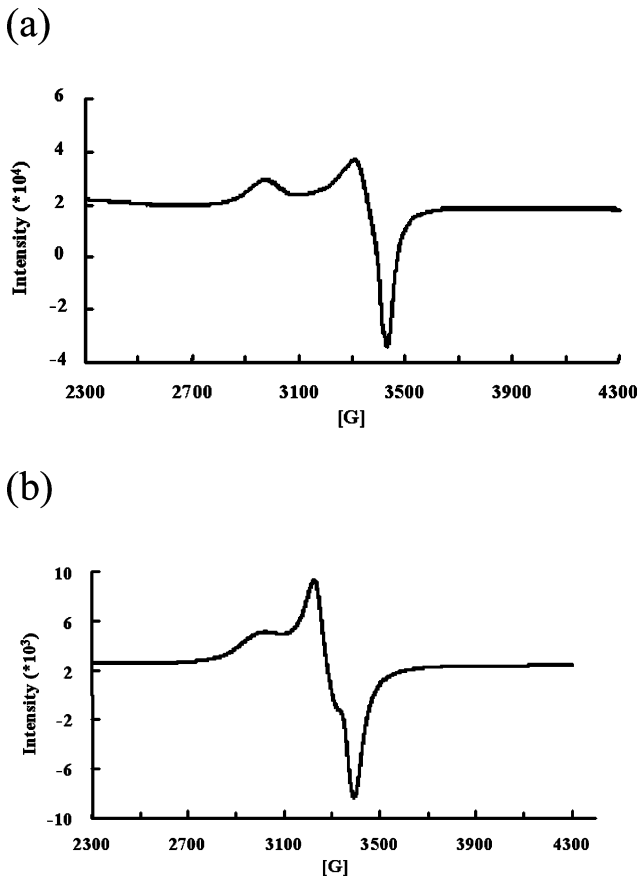

Figure 1. (a) X-band frozen-solution [THF−CH_3CN (3:1 volume ratio)] EPR spectrum of complex **1** with g values of 2.31, 2.04, and 1.99 recorded at 77 K and (b) X-band powdered sample EPR spectrum of complex **1** with g values of 2.28, 2.09, and 2.02.

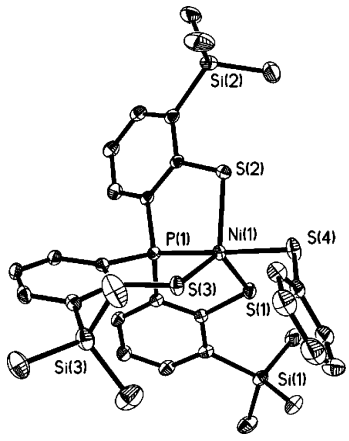

Figure 2. ORTEP drawing and labeling scheme of complex **2** with thermal ellipsoids drawn at the 50% probability level. Selected bond distances (Å) and angles (deg): Ni(1)−S(4) 2.2459(9), Ni(1)−S(1) 2.2986(8), Ni(1)−S(2) 2.2698(9), Ni(1)−S(3) 2.2133(8), Ni(1)−P(1) 2.1375(8); S(4)−Ni(1)−P(1) 176.82(3),S(4)−Ni(1)−S(1)93.16(3),S(4)−Ni(1)−S(2)90.38(4),S(4)−Ni(1)−S(3) 96.11(3),S(1)−Ni(1)−S(2)1.6.92(3),S(2)−Ni(1)−S(3)123.94(4),S(1)−Ni(1)−S(3) 128.06(4).

2 and $[Ni^{III}(SePh)(P(C_6H_3\text{-}3\text{-}SiMe_3\text{-}2\text{-}S)_3)]^-$ dominated by one intense absorption band at 592 and 590 nm, respectively, the electronic spectrum of complex **1** coordinated by the less electron-donating phenoxide ligand displays a red shift to 603 nm (Figure 3).

To further examine the effect of electronic modulations of the monodentate ligand $[OR]^-$ on the stability and

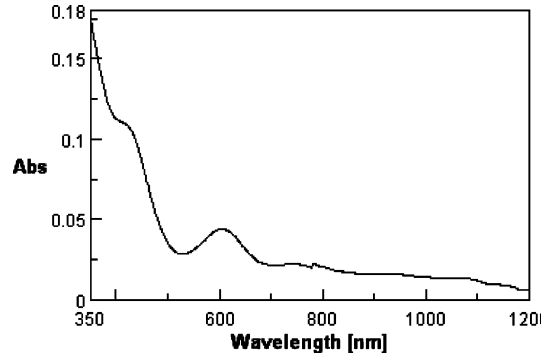

Figure 3. UV−vis spectrum (in THF) of complex **1**.

reactivity of $[Ni^{III}(OR)(P(C_6H_3\text{-}3\text{-}SiMe_3\text{-}2\text{-}S)_3)]^-$ complexes, complex $[Ni^{III}(OMe)(P(C_6H_3\text{-}3\text{-}SiMe_3\text{-}2\text{-}S)_3)]^-$ (**3**) containing the terminal methoxide ligand was synthesized by adopting complex **1** serving as a precursor. In contrast to the reaction of $[Ni^{III}(Cl)(P(C_6H_3\text{-}3\text{-}SiMe_3\text{-}2\text{-}S)_3)]^-$ and [Na][OPh] yielding complex **1** as shown in Scheme 1a, the addition of 1 equiv of [Na][OMe] into a THF−CH_3CN solution of $[Ni^{III}(Cl)(P(C_6H_3\text{-}3\text{-}SiMe_3\text{-}2\text{-}S)_3)]^-$ produced the known Ni^{III} complex $[Ni^{III}(CH_2CN)(P(C_6H_3\text{-}3\text{-}SiMe_3\text{-}2\text{-}S)_3)]^-$ (**4**) characterized by the UV−vis spectrum [characteristic absorptions (543 and 648 nm) for (CH_3CN); Scheme 1b]. These results implicate the electron-deficient $[NiPS_3]$ core induced by the elimination of a NaCl salt from the reaction of $[Ni^{III}(Cl)(P(C_6H_3\text{-}3\text{-}SiMe_3\text{-}2\text{-}S)_3)]^-$ and [Na][OMe] may promote coordination of CH_3CN to the $[NiPS_3]$ core to yield the proposed $[Ni^{III}(NCCH_3)(P(C_6H_3\text{-}3\text{-}SiMe_3\text{-}2\text{-}S)_3)]$ intermediate. The stronger base $[OMe]^-$, compared to $[OPh]^-$, may then trigger deprotonation of the coordinated CH_3CN of the proposed $[Ni^{III}(NCCH_3)(P(C_6H_3\text{-}3\text{-}SiMe_3\text{-}2\text{-}S)_3)]$ intermediate, and the subsequent coordination of the $[CH_2CN]^-$ carbanion to Ni^{III} yields the thermally stable complex **4**.[7]

Upon slow injection of 1 equiv of [n-Bu_4N][OMe] in MeOH into the THF−MeOH solution of complex **1** and after stirring overnight at room temperature, the anionic **3** was isolated as a dark green solid and characterized by single-crystal X-ray diffraction (Scheme 1c). The conversion of complex **1** to complex **3** was monitored by UV−vis spectrometry; the intense absorption bands at 603 and 743 nm disappeared, accompanied by the formation of absorption bands at 599 and 749 nm. The frozen-solution EPR spectrum of complex **3** in THF−CH_3OH (3:1 volume ratio) at 77 K, essentially indistinguishable from those of the 77 K EPR spectra of complexes **1** and **2** (g = 2.31, 2.04, and 1.99 in THF−CH_3CN (3:1 volume ratio) at 77 K), exhibits high rhombicities with three principal g values of 2.28, 2.04, and 2.00 (Figure 4). Compared to complex **2** ($E_{1/2}$ = −1.09 V) and $[Ni^{III}(ER)(P(C_6H_3\text{-}3\text{-}SiMe_3\text{-}2\text{-}S)_3)]^-$ ($E_{1/2}$ = −1.32 V for ER = SEt and $E_{1/2}$ = −1.26 V for ER = SePh), complexes **1** and **3** with the coordinated $[OPh]^-$ and $[OMe]^-$ ligands reveal one reversible $Ni^{III/II}$ redox process at −1.08 V [$E_{1/2}$ (CH_3CN)] and −0.96 V [$E_{1/2}$ (MeOH)] (vs Cp_2Fe/Cp_2Fe^+), respectively (Figure 5). The more anodic redox potential of complexes **1** and **3**, compared to those of complexes **2** and $[Ni^{III}(SEt)(P(C_6H_3\text{-}3\text{-}SiMe_3\text{-}2\text{-}S)_3)]^-$, is ascribed to the weaker electron-donating ability of the coordinated $[OR]^-$ (R = Ph,

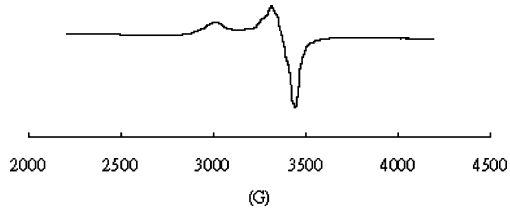

Figure 4. X-band frozen-solution [THF−MeOH (3:1 volume ratio)] EPR spectrum of complex **3** with *g* values of 2.28, 2.04, and 2.00 recorded at 77 K.

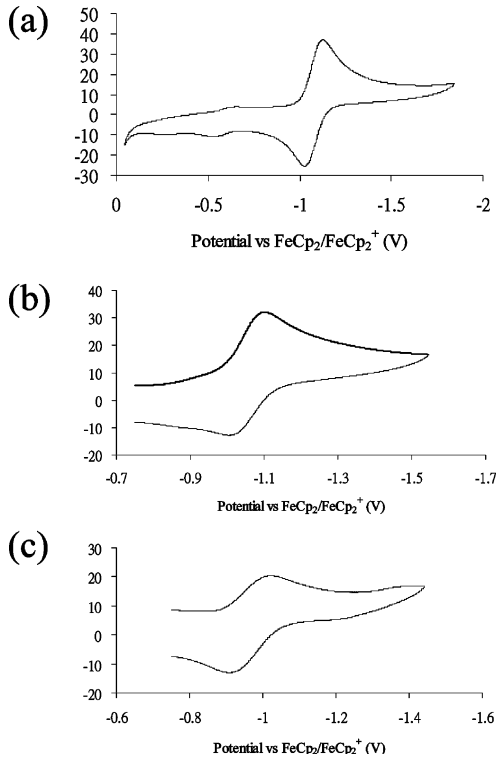

Figure 5. Cyclic voltammograms of (a) a 2.0 mM CH_3CN solution of complex **2**, (b) a 2.0 mM CH_3CN solution of complex **1**, and (c) a 2.0 mM MeOH solution of complex **3** in 0.1 M [*n*-Bu_4N][PF_6] with a glassy carbon working electrode. [Potentials were measured at 298 K vs a Ag/AgCl reference electrode by using a glassy carbon working electrode. Under the conditions employed, the potential (V) of the ferrocinium/ferrocene couple was 0.39 (CH_2Cl_2)].

Me) ligand compared to [SEt]$^-$ and implies the existence of the metastable [Ni^{II}(OR)(P(C$_6$H$_3$-3-SiMe$_3$-2-S)$_3$)]$^{2-}$. Reduction of complex **1** by 1 equiv of [PPN][BH_4] in THF−CH_3CN under N_2 at ambient temperature yielded the proposed [Ni^{II}(OPh)(P(C$_6$H$_3$-3-SiMe$_3$-2-S)$_3$)]$^{2-}$ [UV−vis: 447 and 792 nm (Figure 6)], the analogue of the known [Ni^{II}(PPh$_3$)(P(C$_6$H$_4$-2-S)$_3$)]$^-$,[7b] and then the thermally unstable [Ni^{II}(OPh)(P(C$_6$H$_3$-3-SiMe$_3$-2-S)$_3$)]$^{2-}$ converted into the known [Ni$^{II}_2$(P(C$_6$H$_3$-3-SiMe$_3$-2-S)$_3$)$_2$]$^{2-}$ characterized by UV−vis and single-crystal X-ray diffraction.[7d]

It has been known that the reactivity of [Ni^{III}(L)(P(C$_6$H$_3$-3-SiMe$_3$-2-S)$_3$)]$^-$ may be tailored by ligand L.[7] To further explore the nickel(III) thiolate complexes containing the terminal Ni^{III}−OH bond, we repeated the reaction of complex **1** and [Me_4N][OH] in THF−CH_3OH. On the basis of the UV−vis spectrum and single-crystal X-ray diffraction, complex **3** was isolated after the reaction solution of complex **1** and 1 equiv of [Me_4N][OH] was stirred for 3 h and the insoluble solid was removed.

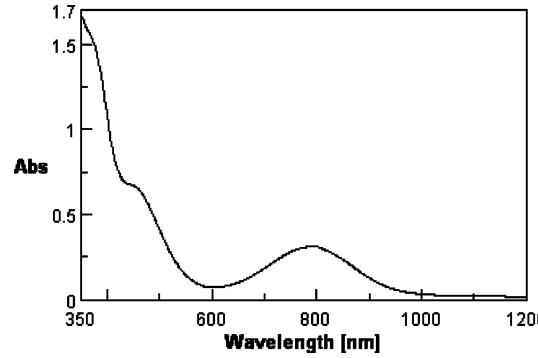

Figure 6. UV−vis spectrum (in THF−CH_3CN) of the proposed [Ni^{II}(OPh)(P(C$_6$H$_3$-3-SiMe$_3$-2-S)$_3$)]$^{2-}$.[7b]

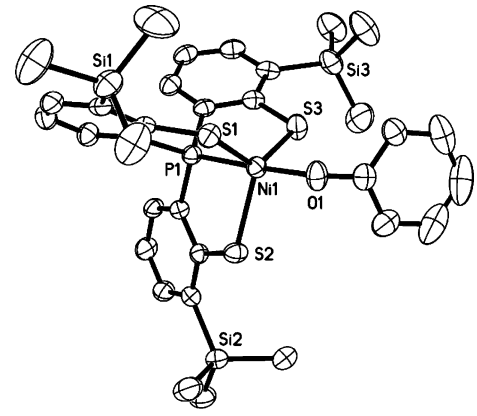

Figure 7. ORTEP drawing and labeling scheme of complex **1** with thermal ellipsoids drawn at the 50% probability level. Selected bond distances (Å) and angles (deg): Ni(1)−O(1) 1.910(3), Ni(1)−S(1) 2.2603(11), Ni(1)−S(2) 2.3191(11), Ni(1)−S(3) 2.2254(11), Ni(1)−P(1) 2.1313(11); O(1)−Ni(1)−P(1) 177.25(10), O(1)−Ni(1)−S(1) 90.39(9), O(1)−Ni(1)−S(2) 97.20(9), O(1)−Ni(1)−S(3) 94.35(8), S(1)−Ni(1)−S(2) 106.04(4), S(2)−Ni(1)−S(3) 122.29(4), S(1)−Ni(1)−S(3) 130.25(5).

Compared to the reported dinuclear bis(*μ*-oxo)nickel(III) complexes [(PhTt^{t}Bu)Ni]$_2$(*μ*-O)$_2$, [Tp^{Me3}Ni(*μ*-O)NiTp^{Me3}], and [Ni$_2$(*μ*-O)(Me$_3$-tpa)$_2$]$^{2+}$,[5] complexes **1** and **3** are the first examples of mononuclear nickel(III) thiolate complexes containing a terminal phenoxide/alkoxide ligand, characterized by single-crystal X-ray diffraction. Single-crystal X-ray structures of complexes **1** and **3** are shown in Figures 7 and 8, respectively, and selected bond lengths and bond angles are collected in the figure captions. The geometry of the Ni center in complex **3** is a distorted trigonal bipyramid, with O(1) and P(1) occupying the axial positions. The Ni−O(R) distances of 1.910(3) and 1.885(2) Å in complexes **1** and **3**, respectively, are comparable to the Ni−O(H) bond distance (1.91 Å) observed in the active-site structure of the oxidized form [NiFe] H_2ase,[2e−g] and similar to the corresponding metrics for dinuclear bis(*μ*-oxo)nickel(III) complexes established by single-crystal X-ray analysis.[5] The shortening of the Ni−OMe bond distance [1.885(2) Å] in complex **3**, compared to the Ni−OPh bond length of 1.910(3) Å in complex **1**, is presumably caused by the stronger electron-donating methoxide ligand coordinating to the electron-deficient Ni^{III} core to stabilize complex **3**. Of importance, in contrast to the Ni−OPh and Ni−OMe bond distances of 1.910(3) and 1.885(2) Å found in **1** and **3**, respectively, the shorter Ni−SPh distance of 2.246(1) Å observed in complex

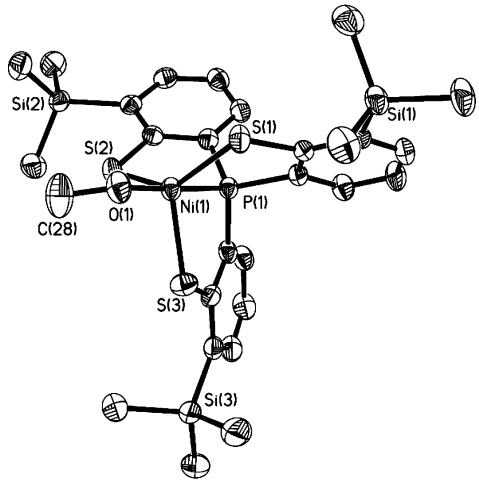

Figure 8. ORTEP drawing and labeling scheme of complex **3** with thermal ellipsoids drawn at the 50% probability level. Selected bond distances (Å) and angles (deg): Ni(1)−O(1) 1.885(2), Ni(1)−S(1) 2.2591(10), Ni(1)−S(2) 2.2988(10), Ni(1)−S(3) 2.2794(10), Ni(1)−P(1) 2.1162(10); O(1)−Ni(1)−P(1) 176.65(8), O(1)−Ni(1)−S(1) 91.35(8), O(1)−Ni(1)−S(2) 100.97(9), O(1)−Ni(1)−S(3) 96.18(9), S(1)−Ni(1)−S(2) 136.15(4), S(2)−Ni(1)−S(3) 105.84(4), S(1)−Ni(1)−S(3) 114.51(4).

Table 1. Selected Bond Length (Å) and Angle (deg) for Complexes **1**−**3**, $[Ni^{III}(SePh)(P(C_6H_3\text{-}3\text{-}SiMe_3\text{-}2\text{-}S)_3)]^-$, and $[Ni^{III}(SEt)(P(C_6H_3\text{-}3\text{-}SiMe_3\text{-}2\text{-}S)_3)]^-$

compound	Ni−ER (E = O, S, Se; R = Ph, Et)	$Ni-S_{ave}$	Ni−P
1	1.910(3)	2.268(1)	2.131(1)
3	1.885(2)	2.279(1)	2.116(1)
2	2.246(1)	2.261(1)	2.138(1)
$[Ni^{III}(SEt)(P(C_6H_3\text{-}3\text{-}SiMe_3\text{-}2\text{-}S)_3)]^-$	2.273(1)	2.253(1)	2.135(1)
$[Ni^{III}(SePh)(P(C_6H_3\text{-}3\text{-}SiMe_3\text{-}2\text{-}S)_3)]^-$	2.347(1)	2.263(1)	2.132(1)

2, compared to the Ni−SEt distance of 2.273(1) Å observed in $[Ni^{III}(SEt)(P(C_6H_3\text{-}3\text{-}SiMe_3\text{-}2\text{-}S)_3)]^-$,[7] may implicate the significant σ and π donation from [SPh] to Ni^{III} (Table 1).[8] Presumably, the tunable electron-donating functionalities of the tetradentate ligand $[P(C_6H_3\text{-}3\text{-}SiMe_3\text{-}2\text{-}S)_3]^{3-}$ of $[Ni^{III}(L)(P(C_6H_3\text{-}3\text{-}SiMe_3\text{-}2\text{-}S)_3)]^-$ modulated by the monodentate ligand L may reimburse the electronic deficiency of the Ni center induced by the less electron-donating ability of the $[OR]^-$ ligand to stabilize the $[Ni^{III}-OR]$ motif.

Conclusion and Comments

Mononuclear **1** containing a terminal [OPh]-coordinated ligand, characterized by UV−vis, EPR, CV, and single-crystal X-ray diffraction, was synthesized from the reaction of $[Ni^{III}(Cl)(P(C_6H_3\text{-}3\text{-}SiMe_3\text{-}2\text{-}S)_3)]^-$ with 3 equiv of [Na][OPh] in THF-CH_3CN (3:1 volume ratio) at room temperature. In the synthesis of mononuclear $[Ni^{III}(OMe)(P(C_6H_3\text{-}3\text{-}SiMe_3\text{-}2\text{-}S)_3)]^-$ containing a terminal $[OMe]^-$ ligand, methoxide [n-Bu_4N][OMe] triggers ligand substitution of complex **1** to yield complex **3**, in contrast to the addition of $[Ni^{III}(Cl)(P(C_6H_3\text{-}3\text{-}SiMe_3\text{-}2\text{-}S)_3)]^-$ into [Na][OMe] producing the known **4** in THF−CH_3CN. These results show that the reaction pathways [ligand-displacement reaction yielding complex **1** (Scheme 1a) vs deprotonation reaction yielding complex **4** (Scheme 1b)] upon the reaction of $[Ni^{III}(Cl)(P(C_6H_3\text{-}3\text{-}SiMe_3\text{-}2\text{-}S)_3)]^-$ and nucleophiles ([Na][OR], R = Ph, Me) in THF−CH_3CN may be regulated by nucleophiles.

At 77 K, complexes **1** and **3** exhibit a rhombic signal with g values of 2.31, 2.09, and 2.00 and of 2.28, 2.04, and 2.00, respectively, the characteristic g values of the trigonal-bipyramidal low-spin d^7 Ni^{III} complexes $[Ni^{III}(L)(P(C_6H_3\text{-}3\text{-}SiMe_3\text{-}2\text{-}S)_3)]^-$ (L = SEt, SePh, Cl, CH_2CN).[7] In contrast to the $Ni^{III}-SPh$ and $Ni^{III}-SEt$ bond distances of 2.246(1) and 2.273(1) Å found in $[Ni^{III}(SR)(P(C_6H_3\text{-}3\text{-}SiMe_3\text{-}2\text{-}S)_3)]^-$ (R = Ph, Et), respectively, the longer terminal $Ni^{III}-OPh$ bond distance of 1.910(3) Å observed in complex **1**, compared to the $Ni^{III}-OMe$ bond length of 1.885(2) Å found in complex **3**, may implicate the absence of the significant σ and π donation from [OPh] to Ni^{III}.[8] Presumably, the electron-rich functionalities of the Ni^{III} center derived from $[P(C_6H_3\text{-}3\text{-}SiMe_3\text{-}2\text{-}S)_3]^{3-}$ acting as a strong σ- and π-donating group in complexes **1** and **3** are responsible for the stabilization of the Ni^{III} state to prevent the reduction of Ni^{III} by the monodentate $[OR]^-$ (R = Ph, Me) ligand. This study unambiguously illustrates the aspect of how the coordinated ligands ($[OR]^-$ and $[P(C_6H_3\text{-}3\text{-}SiMe_3\text{-}2\text{-}S)_3]^{3-}$) of the mononuclear $[Ni^{III}(OR)(P(C_6H_3\text{-}3\text{-}SiMe_3\text{-}2\text{-}S)_3)]^-$ function cooperatively to reach an optimum electronic condition to stabilize the nickel(III) thiolate alkoxide complexes.

Experimental Section

Manipulations, reactions, and transfers were conducted under N_2 according to Schlenk techniques or in a glovebox. Solvents were distilled under N_2 from appropriate drying agents (diethyl ether from CaH_2; acetonitrile from $CaH_2-P_2O_5$; methylene chloride from CaH_2; hexane and THF from sodium benzophenone) and stored in dried, N_2-filled flasks over 4 Å molecular sieves. N_2 was purged through these solvents before use. Solvent was transferred to the reaction vessel via a stainless cannula under a positive pressure of N_2. The reagents $[Na][OC_6H_5]$, [n-Bu_4N][OCH_3], bis(triphenylphosphoranylidene)ammonium chloride ([PPN][Cl]; Fluka), diphenyl disulfide, nickel(II) dichloride, $[(CH_3)_4N][OH]$, and [Na][OMe] were used as received. Compound $[PPN][Ni(Cl)(P(o\text{-}C_6H_3\text{-}3\text{-}SiMe_3\text{-}2\text{-}S)_3)]$ was synthesized by published procedures.[7c] UV−vis spectra were recorded on a GBC Cintra 10e. ^1H NMR spectra were obtained on a Varian Unity-500 spectrometer. Electrochemical measurements were performed with CHI model 421 potentionstat (CH Instrument) instrumentation. Cyclic voltammograms were obtained from 2.0 mM analyte concentration in THF using 0.1 M [n-Bu_4N][PF_6] as the supporting electrolyte. Potentials were measured at 298 K vs a Ag/AgCl reference electrode by using a glassy carbon working electrode. Under the conditions employed, the potential (V) of the ferrocinium/ferrocene couple was 0.39 (CH_2Cl_2). Analyses of C, H, and N were obtained with a CHN analyzer (Heraeus).

Preparation of $[PPN][Ni(OC_6H_5)P(C_6H_3\text{-}3\text{-}SiMe_3\text{-}2\text{-}S)_3]$ (1). Compounds $[PPN][Ni(Cl)P(C_6H_3\text{-}3\text{-}SiMe_3\text{-}2\text{-}S)_3]$ (0.242 g, 0.2 mmol) and $[Na][OC_6H_5]$ (0.070 g, 0.6 mmol) were dissolved in 5 mL of a THF−CH_3CN (volume ratio 3:1) mixture solution in a Schlenk tube under N_2. The reaction solution was stirred for 12 h at ambient temperature, and a solution color change from yellow green to deep green was observed. The blue-shift absorptions from 430 and 620 nm ($[PPN][Ni(Cl)P(C_6H_3\text{-}3\text{-}SiMe_3\text{-}2\text{-}S)_3]$) to 411 and 603 nm implicated the formation of **1**. The mixture solution was

(8) Ashby, M. T.; Enemark, J. H.; Lichtenberger, D. L. *Inorg. Chem.* **1988**, *27*, 191.

filtered through Celite to remove the insoluble NaCl and the excess [Na][OC_6H_5]. Diethyl ether (20 mL) was then added to precipitate the deep-green solid **1** (yield 0.181 g, 73%). Crystals suitable for X-ray diffraction were obtained by layering of a THF−CH_3CN solution of complex **1** and diethyl ether at ambient temperature for 6 days. ^{1}H NMR (C_4D_8O): δ 15.8 (br), 10.4 (br), 9.4 (br), −5.3 (br) ppm ([OC_6H_5]$^-$ and [P(C_6H_3-3-$SiMe_3$-2-S)$_3$]$^{3-}$). Absorption spectrum (THF) [λ_{max}, nm (ϵ, M^{-1} cm^{-1})]: 411 (6700), 603 (2900), 743 (1550), 910 (1100). Anal. Calcd for $C_{69}H_{71}P_3NiOS_3Si_3$: C, 65.65; H, 5.67. Found: C, 65.15; H, 5.70.

Preparation of [PPN][Ni(SC$_6$H$_5$)P(C$_6$H$_3$-3-SiMe$_3$-2-S)$_3$] (2). Compounds [PPN][Ni(Cl)P(C_6H_3-3-$SiMe_3$-2-S)$_3$] (0.242 g, 0.2 mmol) and [Na][SC_6H_5] (0.027 g, 0.2 mmol) were loaded into a 20 mL Schlenk tube and dissolved in 5 mL of a THF−CH_3CN (volume ratio 4:1) mixture solution under N_2. The reaction solution was stirred for 4 h at ambient temperature, and then the mixture solution was filtered through Celite to remove the insoluble NaCl. Diethyl ether (20 mL) was then added to precipitate the green solid **2** (yield 0.175 g, 70%). Crystals suitable for X-ray diffraction were obtained by layering of a THF−CH_3CN solution of complex **2** and diethyl ether at ambient temperature for 6 days. ^{1}H NMR (C_3D_6O): δ 14.8 (br), 10.5 (br), 8.3 (br), −4.0 (br) ppm ([SC_6H_5]$^-$ and [P(C_6H_3-3-$SiMe_3$-2-S)$_3$]$^{3-}$). Absorption spectrum (MeCN) [λ_{max}, nm (ϵ, M^{-1} cm^{-1})]: 357 (7350), 592 (1650), 949 (700). Anal. Calcd for $C_{69}H_{71}P_3NiS_4Si_3$: C, 64.82; H, 5.60. Found: C, 64.49; H, 5.69.

Preparation of [PPN][Ni(OCH$_3$)P(C$_6$H$_3$-3-SiMe$_3$-2-S)$_3$] (3). Complex **1** (0.248 g, 0.2 mmol) was loaded into a 30 mL Schlenk tube, followed by the addition of 5 mL of a THF−CH_3OH (volume ratio 9:1) mixture solvent by a cannula under positive N_2 pressure. A portion of [*n*-Bu_4N][OCH_3] [0.32 mL (20% in CH_3OH solution)] was then added into the THF−CH_3OH solution of complex **1** by syringe. The mixture solution was stirred overnight at room temperature. The mixture solution was filtered through Celite to remove the insoluble [Bu_4N][OC_6H_5], and diethyl ether (20 mL) was then added to precipitate the dark-green solid [PPN][Ni(OCH_3)P(C_6H_3-3-$SiMe_3$-2-S)$_3$] (**3**) (yield 0.127 g, 54%). Dark-green crystals suitable for X-ray diffraction analysis were obtained by layering of the THF−CH_3OH solution of complex **3** and diethyl ether at ambient temperature for 6 days. ^{1}H NMR (C_3D_6O): δ 15.4 (br), 10.4 (br), 9.3 (br), −4.9 (br) ppm ([OCH_3]$^-$ and [P(C_6H_3-3-$SiMe_3$-2-S)$_3$]$^{3-}$). Absorption spectrum (CH_3OH) [λ_{max}, nm (ϵ, M^{-1} cm^{-1})]: 418 (3750), 599 (1400), 749 (800). Anal. Calcd for $C_{64}H_{69}P_3NiOS_3Si_3$: C, 64.80; H, 5.86. Found: C, 64.07; H, 5.76.

Reaction of [PPN][Ni(Cl)(P(C$_6$H$_3$-3-SiMe$_3$-2-S)$_3$)] and [Na][OCH$_3$]. Complexes [PPN][Ni(Cl)(P(C_6H_3-3-$SiMe_3$-2-S)$_3$)] (0.242 g, 0.2 mmol) and [Na][OCH_3] (0.011 g, 0.2 mmol) were dissolved in a THF−CH_3CN [5 mL (volume ratio 3:1)] mixture solution under N_2, and the solution was stirred for 3 h at ambient temperature. The solution color changing from yellow-green to purple was observed. The reaction solution was monitored by UV−vis, and the electronic absorptions (543, 648, and 925 nm) implicated the formation of the known **4**.[7c] The resulting purple solution was filtered through Celite to remove the insoluble NaCl. The filtrate was concentrated under vacuum, and diethyl ether was then added to precipitate the known dark-purple solid **4** (yield 0.186 g, 72%) characterized by UV−vis.[7c]

Reaction of Complex 1 and [(CH$_3$)$_4$N][OH] in THF−CH$_3$OH. The CH_3OH solution of [$(CH_3)_4N$][OH] (0.018 g, 0.2 mmol) was added to the THF−CH_3OH solution [5 mL (volume ratio 3:1)] of complex **1** (0.248 g, 0.2 mmol) under N_2. The mixture solution was stirred for 3 h at ambient temperature, and the solution color change from deep green to dark green was observed. The reaction solution was monitored by UV−vis, and the electronic absorptions (418, 599, and 749 nm) implicated the formation of the complex **3**. The resulting dark-green solution was filtered through Celite to remove the insoluble [$(CH_3)_4N$][OPh]. The filtrate was concentrated under vacuum, and diethyl ether was then added to precipitate the dark-green solid complex **3** (yield 0.186 g, 72%) characterized by UV−vis and X-ray diffraction analysis.

Crystallography. Crystallographic data of complexes **1**−**3** are summarized in Tables S2−S4 in the Supporting Information, respectively. The crystals chosen for X-ray diffraction studies measured 0.30 × 0.18 × 0.07 mm for complex **1**, 0.48 × 0.38 × 0.20 mm for complex **2**, and 0.42 × 0.30 × 0.15 mm for complex **3**, respectively. Each crystal was mounted on a glass fiber and quickly coated in an epoxy resin. Unit-cell parameters were obtained by least-squares refinement. Diffraction measurements for complexes **1**−**3** were carried out on a SMART CCD (Nonius Kappa CCD) diffractometer with graphite-monochromated Mo Kα radiation (λ = 0.7107 Å) and between 2.08 and 25.34° for complex **1**, between 2.08 and 25.34° for complex **2**, and between 2.08 and 25.36° for complex **3**. Least-squares refinement of the positional and anisotropic thermal parameters of all non-H atoms and fixed H atoms were based on F^2. A *SADABS* absorption correction was made.[9] The *SHELXTL* structure refinement program was employed.[10]

EPR Measurements. EPR measurements were performed at the X band using a Bruker EMX spectrometer equipped with a Bruker TE102 cavity. The microwave frequency was measured with a Hewlett-Packard 5246 L electronic counter. X-band EPR spectra of complex **1** in THF−CH_3CN were obtained with a microwave power of 19.78 mW (20.02 mW for complex **3**), a frequency at 9.604 GHz (9.636 GHz for complex **3**), and a modulation amplitude of 0.80 G at 100 kHz.

Acknowledgment. We gratefully acknowledge financial support from the National Science Council of Taiwan. The authors thank Ting-Shen Kuo for single-crystal X-ray structural determinations.

Supporting Information Available: X-ray crystallographic file in CIF format and tables of crystallographic data for the structure determinations of **1**−**3**. This material is available free of charge via the Internet at http://pubs.acs.org.

IC801069T

(9) Sheldrick, G. M. *SADABS, Siemens Area Detector Absorption Correction Program*; University of Göttingen: Göttingen, Germany, 1996.
(10) Sheldrick, G. M. *SHELXTL, Program for Crystal Structure Determination*; Siemens Analytical X-ray Instruments Inc.: Madison, WI, 1994.